Cobalt activation of *Escherichia coli* 5′-nucleotidase is due to zinc ion displacement at only one of two metal-ion-binding sites

Lyle McMILLEN*, Ifor R. BEACHAM† and Dennis M. BURNS*[1]

*School of Biomolecular and Biomedical Science, Faculty of Science, Griffith University, Nathan, Brisbane, Queensland 4111, Australia, and †School of Health Science, Faculty of Health Sciences, Griffith University, PMB 50 Gold Coast Mail Centre, Gold Coast, Queensland 4217, Australia

Escherichia coli 5′-nucleotidase activity is stimulated 30- to 50-fold *in vitro* by the addition of Co^{2+}. Seven residues from conserved sequence motifs implicated in the catalytic and metal-ion-binding sites of *E. coli* 5′-nucleotidase (Asp^{41}, His^{43}, Asp^{84}, His^{117}, Glu^{118}, His^{217} and His^{252}) were selected for modification using site-directed mutagenesis of the cloned *ushA* gene. On the basis of comparative studies between the resultant mutant proteins and the wild-type enzyme, a model is proposed for *E. coli* 5′-nucleotidase in which a Co^{2+} ion may displace the Zn^{2+} ion at only one of two metal-ion-binding sites; the other metal-ion-binding site retains the Zn^{2+} ion already present. The studies reported herein suggest that displacement occurs at the metal-ion-binding site consisting of residues Asp^{84}, Asn^{116}, His^{217} and His^{252}, leading to the observed increase in 5′-nucleotidase activity.

Key words: Co^{2+} activation, consensus sequence, phosphoesterase, sequence motif, zinc metalloenzyme.

INTRODUCTION

Escherichia coli 5′-nucleotidase is a periplasmically localized enzyme [1–3] capable of hydrolysing a broad range of substrates, including all 5′-ribo- and 5′-deoxyribo-nucleotides, uridine diphosphate sugars and a number of synthetic substrates, such as bis (*p*-nitrophenyl) phosphate [4–6]. The enzyme has been shown to contain at least one Zn^{2+} ion following purification, and X-ray crystallographic data [7,8] suggests the presence of two metal-ion-binding sites, designated M1 and M2 [8], in the catalytic cleft (Figure 1). 5′-Nucleotidase activity is stimulated 30- to 50-fold by the addition of Co^{2+} [4,5,9]: this level of activation is much higher than that observed for other zinc metalloenzymes in which the increase in activity following Co^{2+} substitution rarely exceeds 5-fold [10,11]. Significant levels of activation of 5′-nucleotidase are also observed with Mg^{2+} and Mn^{2+} [4–6].

Catalytic site sequence similarity between the *E. coli* 5′-nucleotidase and members of the Ser/Thr protein phosphatase ('Ppase') family has led to 5′-nucleotidase being included in this protein family [8,12]. A consensus sequence consisting of three conserved motifs [Asp-Xaa-His-(≈25)-Gly-Asp-Xaa-Xaa-Asp-(≈25)-Gly-Asn-His-Asp/Glu, where Xaa is any amino acid], which contain residues important for catalytic function and metal-ion binding in the Ser/Thr protein phosphatase family has been suggested [12]. This consensus sequence is found in a wide variety of phosphoesterases [12,13], ranging from vertebrates to eubacteria, including the *E. coli* 5′-nucleotidase. Two additional conserved motifs (Leu/Met-Gly-His-Ser/Tyr and Val-Gly-Gly-His-Ser-Asn/Gln) have been identified in all 5′-nucleotidases and many other phosphoesterases [14], and have also been identified using the structure of kidney bean purple acid phosphatase to guide sequence comparisons [15]. Kidney bean purple acid phosphatase contains a dinuclear Fe(III)/Me(II) centre, where Me can be either Fe or Zn, in which the metal ions play distinct critical roles in hydrolysis [15]. Residues from all five conserved motifs have been implicated in the catalytic and metal-ion-binding sites of the *E. coli* 5′-nucleotidase [8], suggesting a common catalytic strategy for phosphate ester hydrolysis within this diverse group of enzymes.

Seven residues from these motifs in *E. coli* 5′-nucleotidase (Asp^{41}, His^{43}, Asp^{84}, His^{117}, Glu^{118}, His^{217} and His^{252}) were selected for modification using site-directed mutagenesis of the cloned *ushA* gene (Figure 1). Amino acid substitutions were designed to minimize tertiary structural alterations. The resultant seven different mutant proteins were purified and their kinetic and chemical characteristics analysed and compared with those obtained for the wild-type 5′-nucleotidase. These studies suggest a model for activation of *E. coli* 5′-nucleotidase in which divalent metal ions may displace the Zn^{2+} ion at only one of two metal-ion-binding sites; the other metal-ion-binding site retains the Zn^{2+} ion already present. Evidence is presented to support the identity of M2 as the low-affinity metal-ion-binding site at which displacement readily occurs, and of M1 as the high-affinity metal-ion-binding site where displacement rarely, if ever, occurs.

EXPERIMENTAL

Bacterial strains

E. coli K12 strains used in this study were BL21Ω (*hsdS gal* (λ*cIts857 ind1 Sam7 nin5 lacUV5-T7 gene1*) *ansB::str*^{R}) [16,17], CJ236 (*dut ung thi relA;* pCJ105 (*Cm*^{r})) [18] and MV1190 (*Δ*(*lac-proAB*) *thi supE Δ*(*srl-recA*)306::Tn10 (*tet*^{r})*/ F' traD36, proA*$^{+}$*B*$^{+}$*, lacI*^{q}*Z ΔM15*) [18].

Phagemids

The *ushA* expression vector, pLM-2, was constructed by inserting an *ushA*-encoding 1.8 kb PCR-amplified fragment, which had been digested with *Hin*dIII and *Bam*HI into similarly digested pT7-7 [19]. The amplification primer pair used corresponds to nucleotide positions −67 to −46 and 1781 to 1803 [20] (www.genome.wisc.edu/k12.htm) and incorporated add-on sequences to generate these unique sites in the amplified

Abbreviations used: p.p.b., parts per billion; ICP-ES, inductively coupled plasma-emission spectroscopy.

[1] To whom correspondence should be addressed (e-mail dennis.burns@griffith.edu.au).

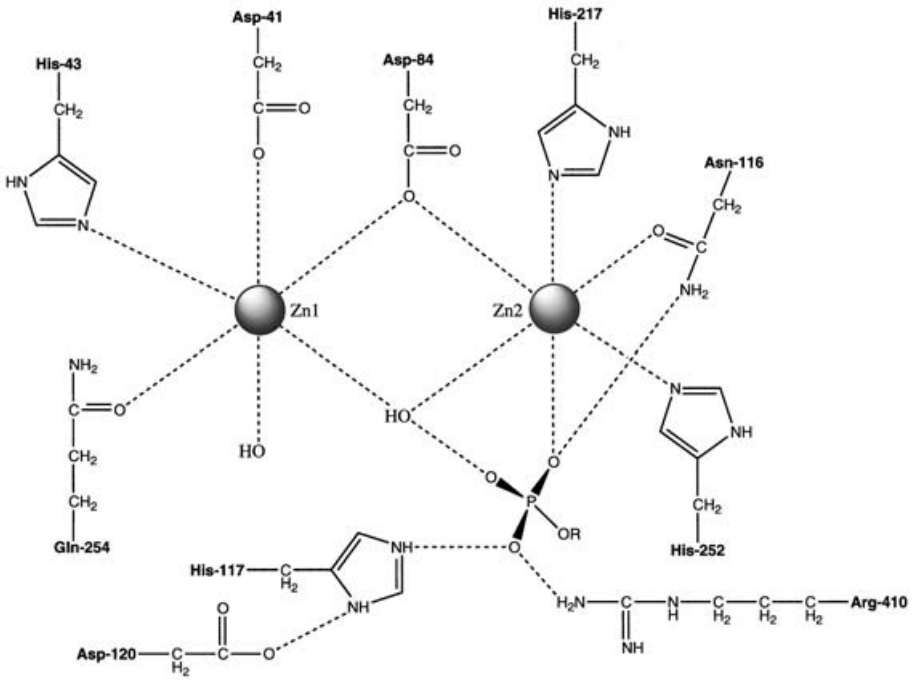

Figure 1 Model of the *E. coli* 5′-nucleotidase metal-ion-binding sites showing ligands coordinating to the two Zn^{2+} ions present during X-ray crystallography

One Zn^{2+} ion, Zn1, occupies binding site M1, and another Zn^{2+} ion, Zn2, occupies binding site M2. This diagram, based on Figure 8(a) from Knöfel and Sträter [27], includes the positions of the mutations referred to in the text with the exception of Glu^{118}, which does not directly form part of either metal-ion-binding site.

product. pLM-3 was made by removing the 1.8 kb *Hin*dIII/*Bam*HI *ushA* fragment from pLM-2 and ligating this into similarly digested pTZ19U [21]. Phagemid derivatives (pLM-4 to pLM-10), each encoding an *ushA* gene-product with a specific amino acid substitution, were generated using oligonucleotide-directed mutagenesis.

PCR

The *ushA* allele was amplified from plasmid pLA7 [22] using oligonucleotides designed to anneal 46 bases upstream of the sequence encoding the initiating methionine codon and 128 nt downstream of the sequence for the *ushA* stop codon [20]. Amplification reactions (50 μl) consisted of 1.5 mM $MgCl_2$, 50 pmol of each primer, 12.5 nmol of dNTP mix (25 mM each of dGTP, dATP, dTTP and dCTP) and 200 pmol of pLA7 that had been purified using a Qiagen plasmid kit. Reactions were placed in a thermal cycler (preheated to 95 °C) for 7 min, prior to the addition of 2.5 units of *Taq* polymerase (Promega). The thermal cycling programme comprised 34 cycles of 95 °C for 1 min, 50 °C for 2 min and 72 °C for 2 min. PCR products were purified from 0.7 % (w/v) agarose gels using QiaEX II resin (Qiagen).

Oligonucleotide-directed mutagenesis

Sequence changes resulting in 5′-nucleotidase derivatives with specific single amino acid substitutions were made using the Muta-Gene phagemid *in vitro* mutagenesis kit, version 2 (Bio-Rad). The change of Asp^{41} (nt 121–123) to Asn was introduced using a 31-mer annealing to the sequence complementary to nt 111–141 of *ushA* [20]. Similarly, six other substitutions were made: His^{43} (nt 127–129) to Asn using a different 31-mer annealing to the sequence complementary to nt 111–141; Asp^{84} (nt 250–252) to Asn using a 30-mer annealing to the sequence complementary to nt positions 235–264; His^{117} (nt 349–351) to Asn using a 30-mer annealing to the sequence complementary to nt 337–366; Glu^{118} (nt 352–354) to Gln using a different 30-mer annealing to nt 337–366; His^{217} (nt 649–651) to Asn using a 25-mer annealing to the sequence complementary to nt 640–664; and His^{252} (nt 754–756) to Asn using a 33-mer annealing to the sequence complementary to nt 736–768. Generation of these mutant derivatives was verified by sequencing of candidate phagemids, using a Big-Dye sequencing kit and a model 377 automated sequencer (Applied Biosystems).

Construction of expression vectors containing *ushA* derivatives with single amino acid changes

The 1.8 kb *Hin*dIII/*Bam*HI fragment from each of the seven phagemids, generated using oligonucleotide-directed mutagenesis, was then ligated into similarly digested pT7–7 to construct a corresponding number of expression vector derivatives (see Table 2) to enable comparative studies of these altered 5′-nucleotidase proteins with the wild-type enzyme. Expression of gene products from *ushA* and of its mutant derivatives, each containing a specific single amino acid substitution, was confirmed by SDS/PAGE and 5′-nucleotidase assay.

Protein purification

Wild-type and mutant 5′-nucleotidases, encoded by pT7–7 plasmid derivatives, were purified as follows. Periplasmic extracts were prepared from 100 ml (3.5 l) of R-broth (10 g/l tryptone, 5 g/l NaCl, 1 g/l glucose and 1 g/l yeast extract) cultures containing 100 μg/ml ampicillin grown aerobically at 37 °C to D_{450} 0.8. The numbers in parentheses indicate the volume changes for larger-scale preparations. The cells were harvested by centrifugation, washed twice with 30 mM Tris/HCl (pH 7.5)/0.3 M NaCl, and

resuspended in 10 ml (140 ml) of a solution containing 40 % (w/v) sucrose/2 mM EDTA/30 mM Tris/HCl (pH 7.5). Lysozyme was added to a final concentration of 0.5 mg/ml and the mixture incubated at 25 °C for 10 min. Spheroplasts were pelleted by centrifugation at 17300 ***g*** for 15 min, and the supernatants (containing the periplasmic fractions) were dialysed at 4 °C against three changes of 1 litre of 5 mM Tris/HCl (pH 7.5) every 2 h. Ion-exchange chromatography was then performed using a BioCAD 700E chromatography system with POROS HQ resin. The proteins were adsorbed to the matrix in 5 mM Tris/HCl (pH 7.5), prior to the application of a 5 mM Tris/HCl (pH 7.5) to 5 mM Tris/HCl (pH 7.5)/200 mM NaCl gradient over 30 column vols. The presence of 5′-nucleotidase in collected fractions was detected by enzyme assay and SDS/PAGE.

Enzyme assay

Assays of 5′-nucleotidase were based on a modification of the method described previously [5]. The assay mixture contained 68 mM sodium acetate (pH 6.0)/13 mM $CaCl_2$/4 mM $CoCl_2$/0.9 mM 5′-AMP in a final volume of 330 μl. P_i was detected by the addition of 0.7 ml of colour-development reagent (10 % ascorbic acid/0.42 % ammonium molybdate in 0.5 M H_2SO_4, 1:6, v/v), followed by incubation at 45 °C for 20 min and measurement of the absorbance at 820 nm. Specific activity was expressed as units/mg of protein, where a unit is defined as the amount of enzyme catalysing the production of 1 μmol of P_i.

Size-exclusion chromatography

Adventitious metal ions were removed from purified 5′-nucleotidase and its mutant derivatives by size-exclusion chromatography using Sephadex G-50 resin (44 cm × 1.5 cm column) at 4 °C with a 2 ml/min flow rate. Prior to use, the matrix was washed with 30 column vols of 5 mM Tris/HCl (pH 7.5) to remove any associated metal ions, and all glassware had been cleaned of metal ions with 10 % (v/v) HNO_3. Buffers were made using distilled deionized water. Protein concentrations of 2–3 mg/ml were loaded on to the column, and 2 ml fractions were collected after 20 ml. Peak active fractions were identified by 5′-nucleotidase assay and SDS/PAGE and stored at − 20 °C until assayed. Prior to metal-ion analysis using inductively coupled plasma-emission spectroscopy (ICP-ES), samples were diluted to 50 μg/ml. Protein concentrations were estimated spectroscopically, with an absorption coefficient at 280 nm of 1.15, based upon a calculated molar absorption coefficient of 66830 $M^{-1} \cdot cm^{-1}$ [23] and a molecular mass of 58134.8 Da [20].

ICP-ES

The concentration in solution of Co^{2+} and Zn^{2+}, in parts per billion (p.p.b.), was determined by ICP-ES analysis, using a SpectroFlame model P + M spectrometer (Analytical Services, Department of Agriculture, University of Queensland, Australia). Standard metal-ion solutions were prepared in the range of 0–300 p.p.b. The detection limit for Co^{2+} has been reported to be 0.4 p.p.b. [24].

RESULTS AND DISCUSSION

Purification of 5′-nucleotidase and its mutant derivatives

Using *E. coli* cultures containing pT7-7 derivatives encoding wild-type 5′-nucleotidase or 5′-nucleotidase variants containing single amino acid substitutions, the protocol described in the present study resulted in the purification, to apparent homogeneity, of 5′-nucleotidase and its mutant derivatives with yields of up to 6 mg of 5′-nucleotidase per litre of original culture. The specific activity of wild-type enzyme was in the range of 670–730 units/mg. Despite the presence of an isopropyl β-D-thiogalactoside-inducible T7 RNA polymerase promoter upstream of the *ushA* gene (or its mutant alleles) in these plasmids, isopropyl β-D-thiogalactoside was found to be unnecessary for high levels of expression (results not shown).

Metal-ion analysis of wild-type enzyme

ICP-ES analyses ($n = 10$) were performed on 50 μg/ml (859 nM) purified wild-type 5′-nucleotidase to determine Zn^{2+}/enzyme molar ratios. Prior to this analysis, the enzyme had been dialysed extensively against 5 mM Tris/HCl (pH 7.5) prepared from distilled deionized water in glassware cleaned with 10 % HNO_3; separate analysis of the buffer determined that the levels of contaminating ions were at, or below, the limits of detection using this procedure (results not shown). Data analysis resulted in a Zn^{2+}/5′-nucleotidase molar ratio of 2.177 ± 0.193:1 (mean ± S.D.). This estimate is consistent with previously reported X-ray crystallography data [8], indicating that two Zn^{2+} ions are associated with *E. coli* 5′-nucleotidase. Interestingly, this is not consistent with the earlier work of Dvorak and Heppel [7] in which a Zn^{2+}/5′-nucleotidase molar ratio of 0.7:1, equating to an estimate of one Zn^{2+} ion per molecule of enzyme, was determined. However, their study involved a multi-step purification procedure performed with the intention of removing any Zn^{2+} not strongly associated with 5′-nucleotidase. Thus this disparity in molar ratios suggests the possibility that at least one of the two metal-ion-binding sites identified by Knöfel and Sträter [8] has a relatively low affinity for Zn^{2+}.

In order to examine potential metal-ion displacement, purified 5′-nucleotidase (1.9 mg/ml) was incubated at 4 °C with or without a 100-fold molar excess of $CoCl_2$, followed by size-exclusion chromatography and subsequent ICP-ES analysis (Table 1). In the absence of added metal ions, Zn^{2+}/enzyme molar ratios in the range of 0.517:1–1.042:1 were obtained (Table 1). Taken with the Zn^{2+}/enzyme molar ratio of 2.177:1 determined for the dialysed sample (see above), the data may be interpreted as indicating the presence of up to two associated Zn^{2+}, but that one of these is more readily dissociated from its binding site. Thus it follows that this binding site has a relatively low affinity for Zn^{2+} ions. Since the Zn^{2+}/enzyme molar ratio was never determined as being lower than 0.5:1 following size-exclusion chromatography,

Table 1 Range of divalent metal ion/wild-type 5′-nucleotidase molar ratios after incubation in the absence or presence of a 100-fold molar excess of metal ions/enzyme

Numbers in parentheses indicate the number of times an experiment was repeated to calculate the range of values. bdl, below the level of detection.

	Molar ratio	
Incubated with	Zn^{2+}/enzyme	Co^{2+}/enzyme
No added $CoCl_2$ or $ZnCl_2$ [0:1]	0.517–1.042:1 (3)	bdl (3)
$CoCl_2$ [100:1]	0.119–0.433:1 (3)	0.385–0.628:1 (3)
$ZnCl_2$ [100:1]	1.525:1 (2)	bdl (2)

this suggests that one Zn^{2+} ion was retained per molecule of enzyme, which, in turn, suggests that the other metal-ion-binding site has a relatively high affinity for Zn^{2+} ions.

The data shown in Table 1 do not conclusively demonstrate displacement of one of two enzyme-associated Zn^{2+} ions by Co^{2+} ions in solution. However, the consistent results of lower Zn^{2+}/enzyme molar ratios for samples incubated with excess Co^{2+} in solution, compared with higher Zn^{2+}/enzyme molar ratios for samples incubated in solution in the absence of added Co^{2+}, suggests a degree of displacement of enzyme-associated Zn^{2+} ions by Co^{2+} ions has occurred. Also, the concomitant detection of, and determined values for, a Co^{2+}/enzyme molar ratio only in samples incubated with excess Co^{2+} in solution is suggestive of at least one Co^{2+} ion per molecule of enzyme. The possibility that these values do not represent a range of Co^{2+}/enzyme molar ratios but rather reflect inefficient removal of Co^{2+} ions in solution by size-exclusion chromatography can be discounted. Control samples containing the same amount of added $CoCl_2$, but no 5′-nucleotidase, were incubated under the same conditions, followed by size-exclusion chromatography and ICP-ES analysis. No significant levels of Co^{2+} were detected in the fractions where 5′-nucleotidase would normally be expected to elute, nor indeed in the surrounding fractions, for any of these control samples (results not shown).

Comparative specific activities of wild-type 5′-nucleotidase and its derivatives containing single amino acid substitutions

Seven residues from the five conserved motifs implicated in enzyme function and/or metal-ion activation were targeted for conservative substitution using site-directed mutagenesis. These residues were Asp^{41}, His^{43}, Asp^{84}, His^{117}, Glu^{118}, His^{217} and His^{252}.

Expression vectors, derived from pT7-7 and encoding each of the seven mutant 5′-nucleotidase proteins and wild-type 5′-nucleotidase (Table 2), were constructed. Following transformation into *E. coli* BL21Ω, all 5′-nucleotidase proteins were purified from these cultures to apparent homogeneity using the described protocol (see the Experimental section) and specific activities determined (Table 2).

The contribution of chromosomally encoded 5′-nucleotidase from *E. coli* BL21Ω to these determined specific activities of purified wild-type and mutant enzymes was clearly negligible, due to overexpression of plasmid-encoded *ushA* gene products. For example, the lowest specific activity in the presence of Co^{2+} was for the 5′-nucleotidase mutant with the $His^{117} \rightarrow Asn$ substitution. Even if the $His^{117} \rightarrow Asn$ mutant was hypothesized to be inactive, and thus the measured activity presumed to represent only chromosomal 5′-nucleotidase, this still represents more than a 2600-fold decrease in activity compared with that of the pLM-2-encoded wild-type 5′-nucleotidase. If, on the other hand, the measured activity mainly represents that of the $His^{117} \rightarrow Asn$ mutant, then the contribution of 'background' chromosomally encoded 5′-nucleotidase becomes even more inconsequential.

Further evidence for low- and high-affinity metal-ion-binding sites

The data presented in Table 2, taken with the X-ray crystallography data relating to the residues involved in metal-ion binding ([8] and Figure 1), support the hypothesis of low- and high-affinity metal-ion-binding sites in *E. coli* 5′-nucleotidase. Asp^{84} is directly involved with both metal-ion-binding sites, and the mutant enzyme encoded by pD84N (Table 2) exhibited both decreased specific activity (>900-fold decrease of the wild-type activity) and increased levels of activation by Co^{2+} (>2700-fold compared with approx. 40-fold for the wild-type). The unusually high level of activation by Co^{2+} exhibited by this $Asp^{84} \rightarrow Asn$ mutant, in comparison with that of other mutants, may be a consequence of loss of the Zn^{2+} ion coordinated by the low-affinity metal-ion-binding site coupled with the decreased affinity of the high-affinity metal-ion-binding site for Zn^{2+}. Mutants exhibiting similar characteristics are proposed to indicate involvement of the corresponding amino acids in the wild-type enzyme in the low-affinity metal-ion-binding site, although levels of activation by Co^{2+} are not expected to be as high in other mutants that coordinate to a single metal ion only.

The mutant encoded by pH217N ($His^{217} \rightarrow Asn$) exhibited significantly decreased specific activity (0.23 % of the wild-type) and was activated more than 240-fold by the addition of Co^{2+} or approx. 6-fold the level of activation for wild-type 5′-nucleotidase (Table 2). The mutant encoded by pH252N ($His^{252} \rightarrow Asn$) also exhibited decreased specific activity (21.9 % of the wild-type) and was activated by Co^{2+} more than 170-fold, or approx. 4-fold the level of activation for wild-type 5′-nucleotidase (Table 2). These results suggest that His^{217} and His^{252} form part of a low-affinity metal-ion-binding site in *E. coli* 5′-nucleotidase.

These mutants ($Asp^{84} \rightarrow Asn$, $His^{217} \rightarrow Asn$ and $His^{252} \rightarrow Asn$) clearly differ from the mutants encoded by pD41N ($Asp^{41} \rightarrow Asn$) and pH43N ($His^{43} \rightarrow Asn$) in respect to the relative levels of Co^{2+} activation. Although the $Asp^{41} \rightarrow Asn$ mutant showed decreased specific activity (9.1 % of wild-type), it was activated in the presence of Co^{2+} by approx. 69-fold, or less than 2-fold the level of activation for wild-type 5′-nucleotidase. Similarly,

Table 2 5′-Nucleotidase activities of purified mutant proteins

All plasmids are pT7-7 derivatives. Specific activity in the presence ($+Co^{2+}$) and absence ($-Co^{2+}$) of cobalt. The experiments were repeated ten times to calculate the range of values.

Amino acid substitution	Plasmid	Specific activity (μmol of P_i/min per mg)		Fold activation in presence of Co^{2+}
		$+Co^{2+}$	$-Co^{2+}$	
None (wild-type)	pLM-2	985.38 ± 35.1	24.79 ± 0.868	39.74
$Asp^{41} \rightarrow Asn$	pD41N	89.55 ± 3.48	1.29 ± 0.052	69.42
$His^{43} \rightarrow Asn$	pH43N	7.44 ± 0.223	0.701 ± 0.021	10.61
$Asp^{84} \rightarrow Asn$	pD84N	1.072 ± 0.0375	0.000386 ± 0.0000308	2777.20
$His^{117} \rightarrow Asn$	pH117N	0.369 ± 0.0185	0.0104 ± 0.00052	35.48
$Glu^{118} \rightarrow Gln$	pE118Q	60.5 ± 2.42	0.5778 ± 0.029	104.71
$His^{217} \rightarrow Asn$	pH217N	2.228 ± 0.128	0.0091 ± 0.00032	244.84
$His^{252} \rightarrow Asn$	pH252N	216.04 ± 8.21	1.253 ± 0.0464	172.42

the $His^{43} \rightarrow Asn$ mutant also showed decreased specific activity (0.76% of wild-type) and its magnitude of activation in the presence of Co^{2+} was approx. 10-fold, which equates to approx. 4-fold less than the level of Co^{2+} activation for the wild-type enzyme. This decreased level of activation was not anticipated and may be caused by the substitution of a residue (His^{43}) which may play a key role in the activated catalysis. Nevertheless, these two mutants ($Asp^{41} \rightarrow Asn$ and $His^{43} \rightarrow Asn$) exhibited changes consistent with their involvement in a high-affinity metal-ion-binding site.

His^{117} is not directly involved in metal-ion-binding (although the X-ray crystallography structure indicates that the carbonate ion coordinated to His^{117} is in turn coordinated to both metal ions), but a role in a catalytic Asp–His dyad with Asp^{120} has been proposed [8]. The mutant encoded by pH117N ($His^{117} \rightarrow Asn$) showed markedly decreased specific activity (0.037% and 0.042% of wild-type in the presence and absence of Co^{2+} respectively), but was activated in the presence of Co^{2+} by approx. 35-fold, similar to the 40-fold activation of wild-type (Table 2). This indicates that the residue plays a role in catalytic function, but not in the proposed low-affinity metal-ion-binding site.

The mutant encoded by pE118Q ($Glu^{118} \rightarrow Gln$) exhibited decreased specific activity (6.1% of wild-type), and the level of activation by Co^{2+} was more than 100-fold, or approx. 2.5-fold the level of activation of wild-type by Co^{2+} (Table 2). These results are clearly not similar to those for mutants containing substitutions of residues involved in either the proposed low- or high-affinity metal-ion-binding sites. However, a role for Glu^{118} in the catalytic site appears likely based on the significant decrease in specific activity in the absence of Co^{2+}. It is interesting that a glutamate residue immediately follows the conserved histidine in motif III (equivalent to the *E. coli* 5′-nucleotidase His^{117}) in 17 of the 20 nucleotidases (5′- and 3′-) studied by Innes et al. [14] and in ten of the 16 other phosphoesterases examined by Zhuo et al. [12]. The remaining six phosphoesterases examined have an aspartate residue in the position analogous to the *E. coli* 5′-nucleotidase Glu^{118}, suggesting the acidic side chains are critical to enzyme structure or function.

Model for Co^{2+} activation of 5′-nucleotidase

In view of previous observations [4,5,7–9] and the results reported in the present study, we propose the following model for Co^{2+} activation of *E. coli* 5′-nucleotidase. Co^{2+} ions readily displace the Zn^{2+} ions at the low-affinity metal-ion-binding site M2 (formed by residues Asp^{84}, Asn^{116}, His^{217} and His^{252}), whereas the high-affinity metal-ion-binding site M1 (formed by residues Asp^{41}, His^{43}, Asp^{84} and Gln^{254}), retains the Zn^{2+} ion already present. The question of precisely how the presence of a coordinated Co^{2+} ion, rather than a Zn^{2+} ion, in the M2 metal-ion-binding site of *E. coli* 5′-nucleotidase activates this enzyme remains open.

Recent studies with thermolysin, which has moderately increased activity (2-fold) following Co^{2+} ion substitution of the resident catalytic Zn^{2+} ion [25], suggest one possible mechanism for exogenous Co^{2+} activation of 5′-nucleotidase. According to X-ray crystallographic studies [8], the two resident Zn^{2+} ions in *E. coli* 5′-nucleotidase were found to be in a trigonal bipyramidal conformation, with each Zn^{2+} tetrahedrally coordinated by four protein ligands (see above). In the case of thermolysin, Co^{2+} is proposed to have a five-coordinate geometry, even in the absence of substrate/inhibitor, with two water molecule ligands, whereas Zn^{2+} ligation is presumed to change from a four-coordinate to a five-coordinate geometry during catalysis [25]. This feature of Co^{2+} may contribute to a more stable transition state and enhanced activity towards the substrate. If a similar situation was true of catalysis by 5′-nucleotidase, this would provide the mechanism for activation by Co^{2+}. However, studies with the zinc endopeptidase astacin have shown that a change in active site geometry is not necessarily a consequence of substitution of Zn^{2+} by Co^{2+} [26].

Another possible mechanism for Co^{2+} activation can be hypothesized from recent crystallographic studies using the substrate analogue α,β-methylene-ADP, which have suggested a reaction mechanism for hydrolysis based upon nucleophilic attack by a metal-bound water molecule [27]. It is possible that the substitution of Co^{2+} for Zn^{2+} in the M2 site induces a slight conformational change in the residues that form this metal-binding site, and thus places the attacking nucleophile in a more favourable in-line position for hydrolysis, increasing the rate of catalysis. Such a conformational change could be due to Co^{2+} ions displaying a strong preference for a particular coordination geometry; for example, a square pyramidal coordinate geometry is favoured by pentacoordinate Co^{2+} ions, contrasting with the random distribution of Zn^{2+} pentacoordinate structures between square pyramidal and trigonal bipyramidal [28]. Studies on the zinc endopeptidase astacin have demonstrated a striking correlation between active site geometry and catalytic function in this metalloproteinase [26].

Kinetic evidence in support of the proposed model

The model predicts that the affinity of enzyme for Co^{2+} will drop significantly when amino acid residues that form part of the low-affinity site, but not the high-affinity site, are substituted. K_m (Co^{2+}) values for wild-type 5′-nucleotidase and its seven mutant derivatives were determined (Table 3). Notably, and consistent with the finding reported previously by Neu [5], 5′-nucleotidase activity in the presence of Co^{2+} was found not to conform to Lineweaver–Burk kinetics (results not shown). Thus a standard graphical method of absorbance at 820 nm versus Co^{2+} concentration, to determine the concentration at which the reaction was at half of its maximal value, was used to estimate K_m (Co^{2+}).

Mutant $Asp^{84} \rightarrow Asn$ displayed an increase in K_m (Co^{2+}) from 92.5 μM for the wild-type to 155 μM for the mutant, reflecting a predicted decrease in the number of ligands coordinating the metal ion resident in the low-affinity metal-ion-binding site. In comparison with wild-type, the change in K_m (Co^{2+}) brought about by substituting His^{252} with Asn^{252} [K_m (Co^{2+}) = 164 μM] is comparable with that for the $Asp^{84} \rightarrow Asn$ mutant, supporting the suggestion that His^{252} is also part of the low-affinity metal-ion-binding site.

Table 3 K_m (Co^{2+}) values of wild-type 5′-nucleotidase and its mutant derivatives

Values are presented as means ± S.D. (μM). The experiments were repeated four times to calculate the range of values.

Amino acid substitution	K_m (Co^{2+})
None (wild-type)	92.5 ± 12.6
$Asp^{41} \rightarrow Asn$	81.8 ± 5.8
$His^{43} \rightarrow Asn$	81.8 ± 6.2
$Asp^{84} \rightarrow Asn$	155.0 ± 7.8
$His^{117} \rightarrow Asn$	99.5 ± 5.8
$Glu^{118} \rightarrow Gln$	459.0 ± 27.9
$His^{217} \rightarrow Asn$	95.4 ± 10.2
$His^{252} \rightarrow Asn$	164.0 ± 2.3

The significant decrease in affinity for Co^{2+} for the $Glu^{118} \rightarrow Asn$ mutant [K_m (Co^{2+}) = 459 μM] suggests Glu^{118} may play an indirect role in the low-affinity metal-ion-binding site, possibly through an adjacent residue. The tertiary structure [8] indicates that Glu^{118} is not in close proximity to either coordinated Zn^{2+} ion, although Asn^{116}, His^{117} and Asp^{120} are present in the active site. As noted previously [12,14], glutamic acid or aspartic acid residues occupy positions in other phosphoesterases and 5′-nucleotidases analogous to the *E. coli* 5′-nucleotidase Glu^{118}, suggesting a critical role of these acidic residues in catalysis or structure.

The $His^{217} \rightarrow Asn$ mutant has a K_m (Co^{2+}) of 95.4 μM, almost identical with that of wild-type (92.5 μM). Nevertheless, X-ray crystallography data suggests that, of the residues examined in the present study, His^{217} coordinates to the same metal ion as Asp^{84} and His^{252}, and mutants of both of these residues exhibit characteristics indicative of roles in the low-affinity metal-ion-binding site.

Other mutants ($Asp^{41} \rightarrow Asn$, $His^{43} \rightarrow Asn$ and $His^{117} \rightarrow Asn$) exhibited no significant changes in K_m (Co^{2+}) from the wild-type (Table 3). For Asp^{41} and His^{43}, these results are consistent with the prediction that they form part of the high-affinity metal-ion-binding site and also with the data in Table 2, suggesting that the metal-ion-binding site formed by these two residues as well as by Asp^{84} and Gln^{254} does not play a significant role in metal-ion displacement and activation. The K_m (Co^{2+}) value determined for the $His^{117} \rightarrow Asn$ mutant is consistent with earlier data in the present study and the findings of Knöfel and Sträter [8], suggesting that His^{117} plays no direct role in metal-ion binding.

In summary, analysis of 5′-nucleotidase-specific activities and K_m (Co^{2+}) values of 5′-nucleotidase and of seven mutant derivatives each with a single amino acid substitution suggests that one Zn^{2+} ion coordinates into a high-affinity metal-ion-binding site (M1) formed by residues Asp^{41}, His^{43} and Asp^{84} (and also Gln^{254} based on X ray crystallographic data; see [8]), whereas another Zn^{2+} ion coordinates into a low-affinity metal-binding site (M2) formed by residues Asp^{84}, His^{217} and His^{252} (and also Asn^{116} based on X ray crystallographic data; see [8]). Neither His^{117} nor Glu^{118} are part of either metal-ion-binding site, but Glu^{118} does appear to have some role in catalytic function and/or structure. This data supports a proposed model for Co^{2+} activation of *E. coli* 5′-nucleotidase in which Co^{2+} ions readily displace the Zn^{2+} ion at the low-affinity metal-ion-binding site, M2, leading to increased enzyme activity, whereas the high-affinity metal-ion-binding site, M1, retains the Zn^{2+} ion already present.

We wish thank staff of Analytical Services, Department of Agriculture, University of Queensland, Australia for assistance with ICP-ES. We also acknowledge the assistance of Dr Susan Hamilton and her research group (Department of Biochemistry, the University of Queensland, Australia). We also thank Dr Dianne Keough for critical reading of the manuscript, and Jeff Dyason for his assistance in preparing Figure 1.

REFERENCES

1 Heppel, L. A. (1971) The concept of periplasmic enzymes. In Structure and Function of Biological Membranes (Rothfield, L. I., ed.), pp. 223–247, Academic Press, New York
2 Neu, H. C. (1967) The 5′-nucleotidase of *Escherichia coli*: II. Surface localization and purification of the *Escherichia coli* 5′-nucleotidase inhibitor. J. Biol. Chem. **242**, 3905–3911
3 Yagil, E. and Beacham, I. R. (1975) Uptake of adenosine 5′-monophosphate by *Escherichia coli*. J. Bacteriol. **121**, 401–405
4 Glaser, L., Melo, A., and Paul, R. (1967) Uridine diphosphate sugar hydrolase: purification of enzyme and protein inhibitor. J. Biol. Chem. **242**, 1944–1954
5 Neu, H. C. (1967) The 5′-nucleotidase of *Escherichia coli*: I. Purification and properties. J. Biol. Chem. **242**, 3896–3904
6 Ruiz, A., Hurtado, C., Ribiero, J. M., Sillero, A. and Sillero, M. A. G. (1989) Hydrolysis of bis(5′-nucleosidyl) polyphosphates by *Escherichia coli* 5′-nucleotidase. J. Bacteriol. **171**, 6703–6709
7 Dvorak, H. F. and Heppel, L. A. (1968b) Metallo-enzymes released from *Escherichia coli* by osmotic shock: II. Evidence that 5′-nucleotidase and cyclic phosphodiesterase are zinc metallo-enzymes. J. Biol. Chem. **243**, 2647–2653
8 Knöfel, T. and Sträter, N. (1999) X-ray structure of the *Escherichia coli* periplasmic 5′-nucleotidase containing a dimetal catalytic site. Nat. Struct. Biol. **6**, 448–453
9 Neu, H. C. and Heppel, L. A. (1965) The release of enzymes from *Escherichia coli* by osmotic shock and during the formation of spheroplasts. J. Biol. Chem. **240**, 3685–3692
10 Coleman, J. E. and Vallee, B. L. (1960) Metallocarboxypeptidases. J. Biol. Chem. **235**, 390–395
11 Prescott, J. M., Wagner, F. W., Holmquist, B. and Vallee, B. L. (1985) Spectral and kinetic studies of metal-substituted *Aeromonas* aminopeptidase: nonidentical, interacting metal-binding sites. Biochemistry **24**, 5350–5356
12 Zhuo, S., Clemens, J. C., Stone, R. L. and Dixon, J. E. (1994) Mutation analysis of a Ser/Thr phosphatase. J. Biol. Chem. **269**, 26234–26238
13 Koonin, E. V. (1994) Conserved sequence pattern in a wide variety of phosphoesterases. Protein Sci. **3**, 356–358
14 Innes, D., Beacham, I. R., Beven, C.-A., Douglas, M., Laird, M. W., Joly, J. C. and Burns, D. M. (2001) The cryptic *ushA gene (ushA^c)* in natural isolates of *Salmonella enterica* (serotype Typhimurium) has been inactivated by a single missense mutation. Microbiology **147**, 1887–1896
15 Klabunde, T., Sträter, N., Fröhlich, R., Witzel, H. and Krebs, B. (1996) Mechanism of Fe(III)–Zn(II) purple acid phosphatase based on crystal structures. J. Mol. Biol. **259**, 737–748
16 Studier, F. W. and Moffatt, B. A. (1986) Use of bacteriophage T7 RNA polymerase to direct selective high-level expression of cloned genes. J. Mol. Biol. **189**, 113–130
17 Harms, E., Wehner, A., Jennings, M. P., Pugh, K. J., Beacham, I. R. and Röhm, K. H. (1991) Construction of expression systems for *Escherichia coli* asparaginase II and two-step purification of the recombinant enzyme from periplasmic extracts. Protein Expression Purif. **2**, 144–150
18 Kunkel, T. A., Roberts, J. D. and Zakour, R. A. (1987) Rapid and efficient site-specific mutagenesis without phenotypic selection. Methods Enzymol. **154**, 367–382
19 Tabor, S. and Richardson, C. C. (1985) A bacteriophage T7 RNA polymerase promoter system for controlled exclusive expression of specific genes. Proc. Natl. Acad. Sci. U.S.A. **82**, 1074–1078
20 Burns, D. M. and Beacham, I. R. (1986) Nucleotide sequence and transcriptional analysis of the *E. coli ush*A gene, encoding periplasmic UDP-sugar hydrolase (5′-nucleotidase): regulation of the *ushA* gene, and the signal sequence of its encoded protein product. Nucleic Acids Res. **14**, 4325–4342
21 Mead, D. A., Szczesna-Skopura, E. and Kemper, B. (1986) Single-stranded DNA 'blue' T7 promoter plasmids: a versatile tandem promoter system for cloning and protein engineering. Protein Eng. **1**, 67–74
22 Burns, D. M., Abraham, L. J. and Beacham, I. R. (1983) Characterization of the *ush* gene of *Escherichia coli* and its protein products. Gene **25**, 343–353
23 Gill, S. C. and von Hippel, P. H. (1989) Calculation of protein extinction coefficients from amino acid sequence data. Anal. Biochem. **182**, 319–326
24 Wolnik, K. A. (1988) Inductively coupled plasma-emission spectrometry. Methods Enzymol. **158**, 190–205
25 Kuzuya, K. and Inouye, K. (2001) Effects of cobalt-substitution of the active zinc ion in thermolysin on its activity and active-site microenvironment. J. Biochem. **130**, 783–788
26 Gamis-Ruth, F.-X., Grams, F., Yiallouros, I., Nar, H., Küsthardt, U., Zwilling, R., Bode, W., and Stöcker, W. (1994) Crystal structures, spectroscopic features, and catalytic properties of cobalt(II), copper(II), nickel(II), and mercury(II) derivatives of the zinc endopeptidase astacin. J. Biol. Chem. **269**, 17111–17117
27 Knöfel, T. and Sträter, N. (2001) Mechanism of hydrolysis of phosphate esters by the dimetal center of 5′-nucleotidase based on crystal structures. J. Mol. Biol. **309**, 239–254
28 Maret, W. and Vallee, B. L. (1993) Cobalt as probe and label of proteins. Methods Enzymol. **226**, 52–71

Received 19 November 2002/17 February 2003; accepted 25 February 2003
Published as BJ Immediate Publication 25 February 2003, DOI 10.1042/BJ20021800